Contents

Chapter 1

Weak focusing synchrotron

1.1 Introduction

Application of the principle of phase stability to resonant acceleration goes back to 1944-1945 [1] and led to "synchronous acceleration" and the synchrotron: the rise in the magnetic field that maintains the particle on a constant-radius orbit, and the modulation of the frequency of the oscillating voltage which accelerates it, are in synchronism with the change of the revolution time,

$$f_{RF}(t) = h f_{rev}(t), \quad B(t) = p(t)/q\rho, \quad \rho = \text{constant} \tag{1.1}$$

• Exercise 1.1-1.
1.1-1.a - Build a data file for a single particle tracking in a 90 degree dipole. Bending radius of the reference trajectory: $\rho_0 = 8.42$ m, field set for an energy of 3.6 MeV. Check your data by tracking a particle on the reference arc at ρ_0.
1.1-1.b - Based on that dipole magnet, build a data file for a circular accelerator with the following geometry: four 90 degree dipoles, 4 meter distant from one another. Check your data by tracking a particle on the closed orbit.
1.1-1.c - Assume 3.6 MeV injection in that ring, and 2.94 MeV top energy. Perform a scan of the value of the magnetic field B, from injection $\check{B}$ to top field $\hat{B}$. Plot B and T_{rev} from that scan, as a function of kinetic energy, together with theory.
1.1-1.d - Plot the resulting f_{rev} as well as $B\rho$, as a function of kinetic energy, together with theory. We will need these outcomes for synchronous acceleration in SATURNE 1. •

The RF frequency synchronism (Eq. 1.1) allows maintaining the bunch at an appropriate phase (the "synchronous phase") with respect to the

oscillating voltage when passing the accelerating gap, and by this means, as will be seen, maintain it longitudinally confined (by the mechanism of "phase focusing") about that equilibrium phase (away from the voltage crest as will be seen, by contrast with the isochronous cyclotron method). Synchronous acceleration is simpler in the case of electrons, as frequency modulation is no longer necessary as long as the initial energy is a few MeV ($v/c = 0.9987$ at 10 MeV, $f_{RF}(t) = hf_{rev}(t) \approx$ constant) (for this reason the first proof-of-principle of phase stability used an existing betatron).

A difference with the cyclotron and synchro-cyclotron families is that the accelerated bunch is constrained to follow a fixed orbit (the "closed orbit"). This results from the momentum ramping in synchronism with B(t), as it does in the betatron, so leading to the above $p(t) = qB(t)\rho$, ρ=constant, at all t. This technique dramatically reduces the size of the guiding magnets, leaving a circular accelerator with an annular, or "ring", structure (Figs. 1.1, 1.2).

A corollary is, synchrotrons of greater energy require a ring of greater diameter, yet the width of the magnet string is essentially unchanged, the volume of iron increases linearly with bunch rigidity. By contrast, a [synchro-]cyclotron magnet is a pair of full, massive cylindrical poles; greater energy requires greater radial extent of the gap to follow the necessary increase of the bend field integral (namely, $\oint B\,dl = 2\pi R_{max}\hat{B} = p_{max}/q$ whereas $\hat{B} \approx 1.8$ 2 T) and accordingly of the diameter of the bulky cylinder, thus the volume of iron increases more than quadratically with bunch rigidity.

Another corollary of the pulsed field in the synchrotron, acceleration is cycled (as it is in general the case in a synchrocyclotron, but not always: the RF frequency is fixed if the accelerated particle is ultra-relativistic [2], or if the optics is quasi-isochronous [3], and in that case acceleration can be CW).

The field ramping law B(t) depends on the type of power supply. If the ramping uses a constant electromotive force, then

$$B(t) \propto (1 - e^{-\frac{t}{\tau}}) \approx \frac{t}{\tau}$$

essentially linear. In that case $\dot{B} = dB/dt$ does not exceed a few Tesla/second, thus the repetition rate of the acceleration cycle if of the order of an Hertz. If the magnet winding is part of a resonant circuit the field law has the form

$$B(t) = \frac{\hat{B}}{2}(1 - \cos\omega t)$$

in that case the repetition rate can reach a few tens of Hertz. In both cases anyway B imposes its law and the other quantities characteristic in the acceleration cycle (RF frequency for instance) will follow B(t).

By contrast in a synchrocyclotron, the field is not ramped, acceleration can be as fast as the voltage system allows; an order of magnitude: take 10 kVolts per turn, meaning about 10,000 turns to 100 MeV, at a velocity $v \approx c$ (to make it simple, although usually $v < c$ over part at least of the cycle), an orbit circumference of $\mathcal{C} = 30$ meter, thus the acceleration takes $T = 10^4 \times \mathcal{C}/c \approx 1\,\text{ms}$, potentially a repetition rate of 1 kHz, three orders of magnitude greater compared to the equivalent pulsed synchrotron.

The invention of the synchrotron was a vast breakthrough. The next decades saw the discovery of several fundamental particles, application in many domains of science, medicine, industry : the weak focusing synchrotron allowed colliding particle beams of highest energies on fixed targets in nucleus fission and particle production experiments, it remains an appropriate technology today for the production of cancer-therapy proton beams; in its strong focussing version (Chapter "Synchrotron, Strong Focusing"), the synchrotron has produced the high energy colliders, the brightest X-ray source, cancer-therapy light ion accelerators use that technology.

Transverse beam focusing in the large, high energy, ion synchrotron rings has inherited from the proven cyclotron and betatron method, namely a transverse field index $0 < n = -\frac{R}{B}\frac{\partial B}{\partial R} < 1$ (that was the case in the first example worked on below, the 3 GeV SATURNE 1 synchrotron [4] started in 1957 at Saclay), combined or not with Thomas focusing ("wedge focusing", which was the case in the second example below, the 12 GeV Zero Gradient Synchrotron "ZGS" (n=0) operated at Argonne in 1964-79 [5]).

In this chapter we retain the two examples of SATURNE 1 at Saclay, for exercises, and the ZGS at Argonne, as a "project", for two main reasons:

- it allows playing with two very different weak focusing methods,
- they saw the first developments on spin polarized proton beams, and their acceleration at the ZGS in 1973, this is an opportunity to start exploring spin motion in particle accelerators.

1.2 Transverse motion

We will introduce the matter using as an example the "SATURNE 1" synchrotron (Fig. 1.1), built at Saclay (CEA, France) in 1956-58, operated in 1958-1973. The magnetic structure is $\frac{2\pi}{N}$-symmetric (or "N-periodic"), featuring N identical $\frac{2\pi}{N}$ degree sector dipoles, between which field-free spac-

SBU SUNY PHYS 684
4 Learning Particle Accelerators – A Computer Game

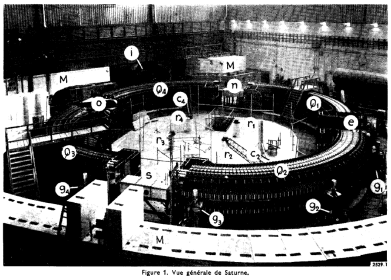

Fig. 1.1 SATURNE 1 at Saclay, France, a 3 GeV, 4-periodic, 68.9 m closed orbit, weak focusing synchrotron ($n \approx 0.6$), started operation in 1957 - plans for polarized proton beams in SATURNE 1 triggered the Froissart-Stora theory of depolarization [6,7]. Each magnet weighs 1150 tons. The four straight sections are 4 m long; injection is in the north one, from a 3.6 MeV Van de Graaff (not visible); the south section houses the extraction system; the RF cavity is in the west one; a beam detection system is located in the east one. The peak power requested from the acceleration RF system does not exceed 2 kW (a "Ham Radio" style of amplifier).

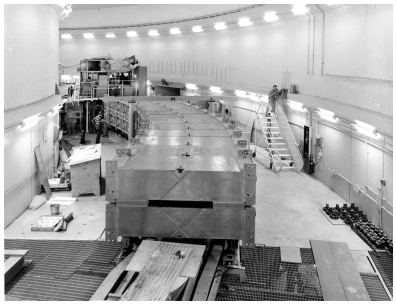

Fig. 1.2 The ZGS at Argonne, IL, USA, during construction, a 12 GeV synchrotron zero-gradient synchrotron, which used wedge focusing (field index zero). ZGS was operated over 1964-1979. First polarized beam acceleration happened at ZGS, in July 1973, to 8.5 GeV/c, up to 12 GeV/c in the following years [7,8]. Pulsed quadrupoles were used to pass through several depolarizing resonances with no significant depolarization, a method known as resonance crossing by fast "tune-jump". Injector: protons from a 20 keV polarized source are pre-accelerated by a 750 keV Cockcroft-Walton, followed by a 50 MeV linac.

ings ("drift space", or "straight section") are introduced. By so "dislocating" a one-piece 360 degree dipole magnet into N identical pieces, the optical structure is changed from one magnetic period per turn, to N periods per turn: the period repeats itself, identically, N times over the ring circumference.

Introducing straight sections in the magnetic structure of the ring allows room for inserting the various systems that garnish the synchrotron: radio-frequency cavity and its voltage gap, injection, extraction, diagnostics systems, special optical elements. This was a similar advantage in the "separated sector" cyclotron, compared to the single-dipole "classical" cyclotron, an outcome of Thomas focusing technique, there.

Motion stability in an axially symmetric dipole field is simply a matter of evaluating the resultant of the forces that apply on the particle, and whether they pull it, both horizontally and vertically, toward the equilib-

rium position, this has been examined earlier ("Cyclotron" Chapter). It is not as simple in the presence of drifts: this lead to introducing two radii (Fig. 1.3):

(i) the magnet curvature radius $\rho_0 = 8.42$ m

(ii) a "physical" radius R = $68.90/2\pi$ = 10.97 m, such that 2πR=circumference=$2\pi\rho_0 + $NL, with L the the length of a drift space.

It also leads to defining a virtual reference line: the theoretical trajectory that a particle of momentum p = qBρ_0 would follow, comprised of arcs of radius ρ_0 in the B-field magnets, and straight lines that connect these arcs.

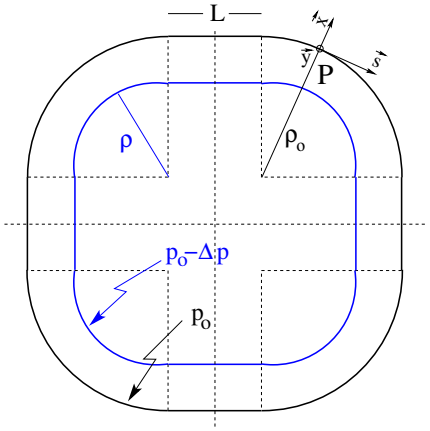

Fig. 1.3 $2\pi/N$ revolution-symmetric structure with drift spaces, and the moving Serret-Frenet frame (s, x, y) attached to the particle at P. The graph shows the reference closed trajectory at momentum p_0 with radius ρ_0 in the bends, and a chromatic orbit for $p = p_0 - \Delta p < p_0$, distant $\Delta x(s) = \frac{\rho_0}{1-n}\frac{\Delta p}{p_0}$.

Parameters of SATURNE 1 weak focusing synchrotron.

Tableau 1. Caractéristiques de Saturne

Rayon magnétique	$r_0 =$	842 cm
Quatre sections droites, chacune de longueur	$l =$	400 cm
Longueur totale de l'orbite d'équilibre ($r = r_0$)	$L =$	6 890 cm
Rayon équivalent	$R_0 =$	1 097 cm
	$=$	1,302 r_0
Index du champ pour $r = r_0$, valeur nominale	$n =$	0,6
Nombre d'oscillations bétatron par tour	$Q_R =$	0,724
	$Q_V =$	0,889
Limite de stabilité		$0{,}50 < n < 0{,}757$
Énergie d'injection	$W_i =$	3,6 MeV
Champ à l'injection	$B_i =$	326 G
Vitesse de montée du champ à l'injection	$(dB/dt)_i =$	20 kG/s
Gain d'énergie par tour pour la particule synchrone	$U_i =$	1 160 V

Fréquence du champ accélérateur (en utilisant l'harmonique $h = 2$ de la fréquence de révolution)	B_0 (kG)	f (MHz)
	0,326	0,760
	10	8,16
	14	8,42
	14,9	8,45
	∞	8,71

Énergie finale	B_0 (kG)	W_f (GeV)
	10	1,76
	14	2,72
	14,9	2,94

Cycle de fonctionnement $\tau = 5{,}2$ s	montée	= 0,9 s
	descente	= 0,9 s
	repos	= 1,4 s
Pression de fonctionnement	$p =$	$5 \cdot 10^{-6}$ mmHg

• Exercise 1.2-1 We will construct SATURNE 1 ring, to end up, in the foregoing, simulating a complete acceleration cycle. First, fill up a spreadsheet with SATURNE 1 parameters as available from the Table on page 5 . Be prepared to complete that spreadsheet with additional parameters as we progress with the simulations. •

• Exercise 1.2-2

Start from Exercise 1.1-1 to complete SATURNE 1, using its parameter list: introduce the field index (assume $n = 0.6$ at $r = r_0$, nominal index at SATURNE 1); set the reference closed orbit (the zero of the reference particle transverse coordinates) on the nominal magnetic radius $r_0 = 8.42$ m; check the general parameters out of the simulation against the data table: circumference, time of flight.
Scan the chromatic orbits over the range $\Delta p = \pm 10^{-3} p_0$, step 10^{-4}, plot $\Delta x/(\Delta p/p_0)$ as a function of Δp, deduce the corresponding value for the field index. •

1.2.1 *Equations of motion in a dipole magnet*

The differential equations in the moving frame (the Serret-Frenet frame, tangent to the reference orbit, Fig. 1.3) for small motion around the trajectory at constant radius ρ_0 are derived from the Lorentz equation,

$$\frac{dm\tilde{v}}{dt} = q\tilde{v} \times \tilde{B} \rightarrow m\frac{d}{dt}\begin{Bmatrix} \frac{ds}{dt}\vec{s} \\ \frac{dx}{dt}\vec{x} \\ \frac{dy}{dt}\vec{y} \end{Bmatrix} = q\begin{Bmatrix} (\frac{dx}{dt}B_y - \frac{dy}{dt}B_x)\vec{s} \\ -\frac{ds}{dt}B_y\vec{x} \\ \frac{ds}{dt}B_x\vec{y} \end{Bmatrix} \qquad (1.2)$$

A "hard-edge" model of a dipole is assumed here: $B_s = 0$, the field falls abruptly to zero at magnet ends. Introduce the field index $n = -\frac{\rho_0}{B_0}\frac{\partial B_y}{\partial x}$ evaluated at $(\rho_0 + x,\ y = 0)$ (so, in passing, B_0 is a short notation for $B_y(\rho_0, y = 0)$) and assume radial and axial stability, $0 < n < 1$. Taylor expansion of the field in the coordinates write

$$B_y(\rho) = B_y(\rho_0) + x\frac{\partial B_y}{\partial x}|_{\rho_0} + \mathcal{O}(x^2) \approx B_y(\rho_0) - n\frac{B_y}{\rho_0}|_{\rho_0}x = B_0(1 - n\frac{x}{\rho_0})$$
$$B_x(0 + y) = \underbrace{B_x(0)}_{=0} + y\ \underbrace{\frac{\partial B_x}{\partial y}}_{=\frac{\partial B_y}{\partial x}} (+\text{higher order in y}) \approx -n\frac{B_0}{\rho_0}y \qquad (1.3)$$

Introduce in addition $ds \approx v dt$ and the deviations with respect to the reference (closed) orbit. In these hypotheses, the differential equations of motion write

$$\frac{d^2x}{ds^2} + \frac{1-n}{\rho_0^2}x = 0, \qquad \frac{d^2y}{ds^2} + \frac{n}{\rho_0^2}y = 0 \quad (0 < n = -\frac{\rho_0}{B_0}\frac{\partial B_y}{\partial x} < 1) \qquad (1.4)$$

1.2.2 *Betatron motion, periodic stability*

The focusing forces take different forms, depending on the type of optical element traversed, namely with index $n \begin{cases} = 0 & \text{in drift spaces} \\ \in]0,1[& \text{in dipole sector} \end{cases}$. However,

the equation of motion, *Hill's equation*, presents the general form

$$\frac{\mathrm{d}^2\mathrm{z}}{\mathrm{ds}^2} + \mathrm{K_z(s)z} = 0 \quad \text{with} \quad \begin{cases} \text{dipole} : \begin{cases} K_x = \frac{1-n}{\rho_0^2} \quad (n = -\frac{\rho_0}{B_0}\frac{\partial B_y}{\partial x}) \\ \mathrm{K_y} = \frac{\mathrm{n}}{\rho_0^2} \end{cases} \\ \text{drift space } (\rho \to \infty) : \mathrm{K_x} = \mathrm{K_y} = 0 \\ \epsilon\text{-angle wedge} : \mathrm{K}_{\substack{x \\ y}} = \pm\frac{\tan\epsilon}{\rho_0} \end{cases} \tag{1.5}$$

$\mathrm{K_z(s)}$ is periodic, its period is that of the ring structure. If S is the length of a period (or "cell") then $\mathrm{K_z(s+S)} = \mathrm{K_z(s)}$ (the length S of a cell is a quarter of the circumference, in SATURNE 1).

Stability of the periodic motion

The solution of Hill's equation can be written under matrix form, a matrix which transports coordinates from entrance to exit of an optical sequence,

$$\mathrm{T_A} = \mathrm{T(S_A + S \leftarrow S_A)} = \begin{bmatrix} \mathrm{T_{11}} & \mathrm{T_{12}} \\ \mathrm{T_{21}} & \mathrm{T_{22}} \end{bmatrix} \quad \text{and} \quad \begin{bmatrix} z \\ z' \end{bmatrix}_{\mathrm{out}} = \mathrm{T_A} \times \begin{bmatrix} z \\ z' \end{bmatrix}_{\mathrm{in}} \tag{1.6}$$

• Exercise 1.2.2-1.
1.a - Compute the transport matrix of SATURNE periodic cell (take n = 0.6). Verify that its determinant has value 1. This results from Liouville's theorem.
1.b - Verify that its trace is independent of the origin of the cell: take the origin at either center of drift, entrance of dipole or center of dipole, compute the different matrices.
1.c - Show, for two of the different origins in (ii), say, $\mathrm{s_A}$ and $\mathrm{s_B}$, that the matrices satisfy $\mathrm{T_B} = \mathrm{U} \times \mathrm{T_A} \times \mathrm{U}^{-1}$, with U the transfer matrix from $\mathrm{s_A}$ to $\mathrm{s_B}$, compute U for 3 different origins: center of drift, entrance or center of dipole).

• Exercise 1.2.2-2. Motion stability (1/3):
The stability (or instability) of particle motion around the ring can be observed by recording the amplitudes x(n), x′(n) and y(n), y′(n) at a fixed azimuth s in the ring, at successive turns for a large number of turns, n.
Accelerator physicists have a predilection for phase space, let's go there: for a particle with small initial horizontal and vertical coordinates, observed at the center of a drift over tens of turns, plot both horizontal and vertical particle motions in their respective phase spaces, (x, x′) and (y, y′). Do it at center of drift and entrance of dipole. What do you observe? •

An other way to study the periodic stability relies on the Twiss notation for the transfer matrix of a period,

$$\mathrm{T(s+S \leftarrow s)} = \begin{bmatrix} \cos\mu + \alpha(\mathrm{s})\sin\mu & \beta(\mathrm{s})\sin\mu \\ -\gamma(\mathrm{s})\sin\mu & \cos\mu - \alpha(\mathrm{s})\sin\mu \end{bmatrix} = \mathrm{I}\cos\mu + \mathrm{J(s)}\sin\mu \tag{1.7}$$

with I =identity matrix and $\mathrm{J}^2 = -\mathrm{I}$. This notation introduces three quantities:

- μ, which satisfies $\cos\mu = \frac{1}{2}\mathrm{Trace(T)}$, the phase advance of the betatron motion, a quantity independent of the origin of the period. The number of betatron oscillations over a period is the

$$\text{betatron wave number of a period :} \quad \nu = \mu/2\pi \tag{1.8}$$

The phase advance over an N-period turn is $\mathrm{N}\mu$ (N = 4 for SATURNE 1) and the wave number per turn is $\mathrm{N}\mu/2\pi$.

Obviously, periodic stability requires

$$-1 < \frac{1}{2}\mathrm{Trace(T)} < 1 \tag{1.9}$$

Note: if $\frac{1}{2}\mathrm{Trace(T)} = 1$, $\frac{\mathrm{d}^2\mathrm{y}}{\mathrm{ds}^2}$ has one solution S-periodic (stable) and one solution linear in s; if $\frac{1}{2}\mathrm{Trace(T)} = 1$, $\frac{\mathrm{d}^2\mathrm{y}}{\mathrm{ds}^2}$ has one solution 2S-periodic (stable) and one solution linear in s; in both cases the resultant is unstable.

- the betatron function β(s), which relates to the amplitude of the betatron oscillations,

- and its derivative $\alpha(\mathrm{s}) = -\frac{1}{2}\frac{\mathrm{d}\beta(\mathrm{s})}{\mathrm{ds}}$.

α(s) and β(s) are S-periodic, a periodicity imposed by $\mathrm{T(s + kS + S \leftarrow s + kS) = T(s + S \leftarrow s)}$, k arbitrary integer.

• Exercise 1.2.2-3. Theoretical properties of the Twiss matrix:
3.a - write explicitly the matrix J(s), calculate J^2,
3.b - what is the value of the matrix T determinant? Deduce the relationship between α(s), β(s) and γ(s),
3.c - show that the transfer matrix T^N over an N-period sequence is obtained by just updating the phase advance: $\mu \rightarrow \mathrm{N}\mu$. •

• Exercise 1.2.2-4. Motion stability (2/3):
4.a - it is a feature of any accelerator optics code to provide the optical functions α(s), β(s) and the phase advance μ. Get these from the computation of SATURNE 1 optical properties.
4.b - back to the observed horizontal and vertical motions of Exercise 1.2.2-2: check that the horizontal motion coordinates recorded after n turns in

the N = 4 cell SATURNE 1 ring satisfy $\begin{pmatrix} x \\ x' \end{pmatrix} = T(nN\mu) \times \begin{pmatrix} x_0 \\ x'_0 \end{pmatrix}$ with $x_0,\ x'_0$ the starting coordinates, $T(nN\mu)$ the Twiss matrix (Eq. 1.7) taken for $\mu \to nN\mu$
4.c - repeat for y, y′, vertical motion,
4.d - plot a few tens of turns in the normalized phase space $(\frac{x}{\sqrt{\beta}}, \frac{\alpha x+\beta x'}{\sqrt{\beta}})$. What is the shape of the trajectory in that phase space? What is the property of the quantity $\frac{x^2}{\beta}, \frac{(\alpha x+\beta x')^2}{\beta}$)?
Check that the progression of the betatron phase from one turn to the next is $N\mu$. •

• Exercise 1.2.2-5. Motion stability (3/3):
5.a - track a particle of initial coordinates $(x_o, x'_0))$ for a few hundred turns around the ring. Record it coordinates a some azimuth, for instance the middle of a drift. Plot these in the transverse horizontal phase space (x, x').
5.b - match this trajectory with an ellipse of equation

$$\gamma_x x^2 + 2\alpha_x x x' + \beta_x x'^2 = \epsilon/\pi \tag{1.10}$$

Compare the values for α_x, β_x, γ_x so obtained with those obtained from the Twiss notation method. What is the relationship between these three quantities?
5.c - repeat this coordinate recording and ellipse matching at the center of the dipole, and at both ends of the drift. Conclusion?
5.d - represent the phase space ellipse of Eq. 1.10 in an (x,x') frame: in terms of α_x, β_x and γ_x, indicate the coordinates of the remarkable points of the ellipse: maximum excursion x_{max}, maximum angle x'_{max}, intersection with the axes: angle at zero excursion $x'(x = 0)$, excursion at zero angle $x(x' = 0)$. What does ϵ_x represent? •

Stability diagram

The "working point" of the synchrotron is the couple (ν_x, ν_y) at which the accelerator is operated, it fully characterizes the focusing (Fig. 1.4). In a structure with revolution symmetry such as the classical cyclotron, we found

$$\nu_x = \frac{\omega_x}{\omega_{rev}} = \sqrt{1-n}, \quad \nu_y = \frac{\omega_x}{\omega_{rev}} = \sqrt{n} \ \text{ thus } \ \nu_x^2 + \nu_y^2 = 1 \tag{1.11}$$

with $\omega_{x,y}$ the radial and axial frequencies of the betatron motion around the ring. Thus when the index is changed the working point stays on a circle

of radius 1 in the stability diagram (or "tune diagram", Fig. 1.4). In a structure with revolution symmetry and drift spaces, such as SATURNE 1, in a first approximation

$$\nu_x = \sqrt{(1-n)\frac{R}{\rho_0}}, \quad \nu_y = \sqrt{n\frac{R}{\rho_0}}, \quad \text{thus} \quad \nu_x^2 + \nu_y^2 = R/\rho_0 \tag{1.12}$$

thus the working point is located on the circle of radius $\sqrt{R/\rho_0} > 1$, for all n (n was changing for instance during acceleration at SATURNE 1). Note that in either case, horizontal and vertical focusing are not independent: if ν_x increases ν_y decreases, and reciprocally, a lack of flexibility - which strong focusing will overcome by providing two knobs, for two independent indices instead (Chapter Synchrotron, Strong Focusing).

• Exercise 1.2.2-6. Here we vary the betatron frequency of paraxial particle motion, by taking different values for n.
6.a - On a common graph superimpose the betatron wave number $\nu_x(n)$, same for $\nu_y(n)$, obtained in three different ways:

- Fourier analysis of the recorded motion in Exercise 1.2.2-2
- using $\cos\mu = \frac{1}{2}\text{Trace(T)}$, with T computed from 1-turn mapping (Eq. 1.9).
- the relationships $\nu_x(n)$, $\nu_y(n)$ of Eq. 1.12.

6.b - Plot these data in a tune diagram. •

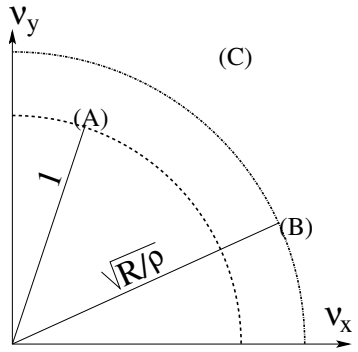

Fig. 1.4 The working point in the tune diagram is located (A): case of revolution symmetry, on a circle of radius 1; (B): case of revolution symmetry + drift spaces, on a circle of radius ($\sqrt{R/\rho_0}$); (C): case of strong focusing, ($|n| \gg 1$), in large ν_x, ν_y regions.

1.2.3 *Off-momentum motion*

The transverse motion of a particle with momentum $p = p_0 + \Delta p$ satisfies

$$\frac{d^2x}{ds^2} + K_x x = \frac{1}{\rho_0}\frac{\Delta p}{p_0}, \qquad \frac{d^2y}{ds^2} + K_y y = 0 \tag{1.13}$$

with K_x, K_y depending on the nature of the optical element:

$$\begin{aligned}
&\diamond \text{ dipole :} && \begin{cases} K_x = \frac{1-n}{\rho_0^2} \quad (n = -\frac{\rho_0}{B_0}\frac{\partial B_y}{\partial x}) \\ K_y = \frac{n}{\rho_0^2} \end{cases} \\
&\diamond \text{ dipole wedge angle :} && \begin{cases} K_{\substack{x \\ y}} = \pm\frac{\tan\epsilon}{\rho_0}\delta(s-s_0) \ (\epsilon \lessgtr 0 \text{ for a } \substack{\text{focusing} \\ \text{defocusing}} \text{ wedge}) \\ \frac{1}{\rho_0} = 0 \end{cases} \\
&\diamond \text{ drift space :} && K_x = K_y = 0 \text{ and } \tfrac{1}{\rho_0} = 0
\end{aligned} \tag{1.14}$$

Just as there exists a closed orbit for the on-momentum particle ($\Delta p = 0$), it results from these considerations that there exists a closed orbit for an off-momentum particle, a "chromatic closed orbit", which closes on itself over a turn and has the periodicity of the ring.

The solution of Eq. 1.13 for any optical element (dipole, wedge, drift) writes under the general form

$$\begin{pmatrix} x_2 \\ x_2' \\ y_2 \\ y_2' \\ \delta \end{pmatrix} = \begin{pmatrix} C_x & S_x & 0 & 0 & D_x \\ C_x' & S_x' & 0 & 0 & D_x' \\ 0 & 0 & C_y & S_y & 0 \\ 0 & 0 & C_y' & S_y' & 0 \\ 0 & 0 & 0 & 0 & 1 \end{pmatrix} \begin{pmatrix} x_1 \\ x_1' \\ y_1 \\ y_1' \\ \delta \end{pmatrix} \tag{1.15}$$

wherein $(*)' = d(*)/ds$, $\delta = (p - p_0)/p_0$, the index 1 (resp. 2) designates the particle coordinates at entrance (resp. exit) of the optical section. In virtue of Eq. 1.14 only the dipole has non-zero chromatic coefficients D_x and D_x': the other elements (drift, wedge) have the right hand side term of Eq. 1.13 zero, thus their D_x and D_x' coefficients are zero.

• Exercise 1.2.3-1. Compute the 5×5 matrices of the cell drift and of the cell dipole (n=0.6) in SATURNE 1, from ray-tracing. Verify that

(i) they have the expected form given in Eq. 1.15 ;

(ii) their coefficient values satisfy, respectively,

$$\text{drift :} \begin{cases} C_x = 1;\ S_x = s - s_0;\ D_x = 0 \\ C_y = 1;\ S_y = s - s_0 \end{cases}$$

$$\text{dipole :} \begin{cases} C_x = \cos\sqrt{K_x}(s-s_0);\ S_x = \frac{1}{\sqrt{K_x}}\sin\sqrt{K_x}\mathcal{L};\ D_x = \frac{1}{\rho_0 K_x}(1 - \cos\sqrt{K_x}(s-s_0)) \\ C_y = \cos\sqrt{K_y}(s-s_0);\ S_y = \frac{1}{\sqrt{K_y}}\sin\sqrt{K_y}(s-s_0) \end{cases}$$

•

• Exercise 1.2.3-2. An illustration that not only the individual optical element matrices (drift, dipole, etc., previous exercise), but as well the global matrix of a sequence of optical elements has the very form given in Eq. 1.15 :
Calculate the analytical expression of the product $\mathrm{T_{dipole}} \times \mathrm{T_{drift}}$ of the drift-dipole cell. Verify that

(i) it has the expected form given in Eq. 1.15 ;

(ii) it yields numerical values which are in accord with the numerical values obtained from the ray-tracing. •

Periodic dispersion, chromatic closed orbit

The chromatic closed orbit satisfies

$$\begin{pmatrix} \mathrm{x_{ch}} \\ \mathrm{x'_{ch}} \\ \delta \end{pmatrix} = \begin{pmatrix} \mathrm{C} & \mathrm{S} & \mathrm{D} \\ \mathrm{C'} & \mathrm{S'} & \mathrm{D'} \\ 0 & 0 & 1 \end{pmatrix} \begin{pmatrix} \mathrm{x_{ch}} \\ \mathrm{x'_{ch}} \\ \delta \end{pmatrix}$$

• Exercise 1.2.3-3. Solve the equation above for $\mathrm{x_{ch}}$, $\mathrm{x'_{ch}}$. Calculate the numerical values of $\mathrm{x_{ch}}/\delta$ and $\mathrm{x_{ch}}/\delta$ they yield in the case of SATURNE period (use the results of exercise 1.2.3-2).

• Exercise 1.2.3-4. Ray-trace in SATURNE cell: verify numerically the value of $\mathrm{x_{ch}}/\delta$ and $\mathrm{x_{ch}}/\delta$ by searching a chromatic closed orbit, say for $\delta = 10^{-3}$. Repeat for the ring (4 cell sequence) - conclusion?

1.3 Acceleration

In a synchrotron, the field B is varied (a function performed by the power supply) as well as the bunch momentum p (a function performed by the accelerating cavity) in such a way that at any time $\mathrm{B(t)}\rho = \mathrm{p(t)/q}$ (ρ is the curvature radius of the "central" or "reference" trajectory, or "machine axis", in the bending magnets). Given the energies involved and as a consequences the ensuing inertia, the magnet supply imposes its law and the cavity follows B(t) law the best in can. A schematic B(t) law is represented in Fig. 1.5.

• Exercise 1.3-1.
Carrying on with SATURNE ring, page 5, fill up your spreadsheet with the additional following data:

$\dot{B}$	T/s	
max. B	T	
ρ	m	
max. Bρ	T/s	

1.3.1 *Energy gain, $\dot{B}$, frequency law*

The energy increase by the cavity follows the field variation in the guiding magnets, $\dot{B} = dB/dt$. The variation of the particle energy over a turn, under the effect of the force on the charge at the cavity, writes

$$\Delta W = F \times 2\pi R = 2\pi q \rho R \dot{B}$$

Over most of the accelerating cycle in a synchrotron, $\dot{B}$ is usually constant, thus ΔW is also a constant. In general, kVolts are applied in smaller size synchrotrons, and 100s of kVolts to MVolts are applied, possibly using several RF stations, in large rings.

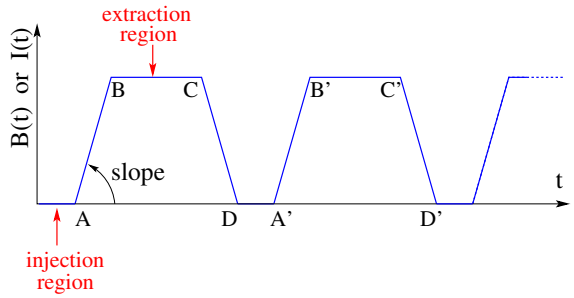

Fig. 1.5 Cycling B(t) in a pulsed synchrotron. Ignoring saturation, B(t) is proportional to power supply I(t). Bunch injection occurs at low field, in the region of A, extraction occurs at top energy, on the high field plateau. (AB): field ramp up; (BC): flat top; (CD): ramp down; (DA'): thermal relaxation. (AA'): repetition period; (1/AA'): repetition rate; *slope*: ramp velocity $\dot{B} = dB/dt$ (Tesla/s).

• Exercise 1.3.2-1.
In SATURNE ring,
1.a - ramp the field in the dipoles to synchronize to a constant increase in energy of the particle, see parameter table in page 5. Use a (artificially) extremely law frequency cavity so to ensure same longitudinal boost at all passes (no synchrotron motion for the moment).
1.b - plot Bρ [T.m] as a function of kinetic energy [MeV], from tracking and from theory.

1.3.2 *Adiabatic damping*

As a result of the longitudinal acceleration at the cavity, the amplitude of betatron oscillations decreases. The mechanism is sketched in Fig. 1.6. Coordinate transport through the cavity writes

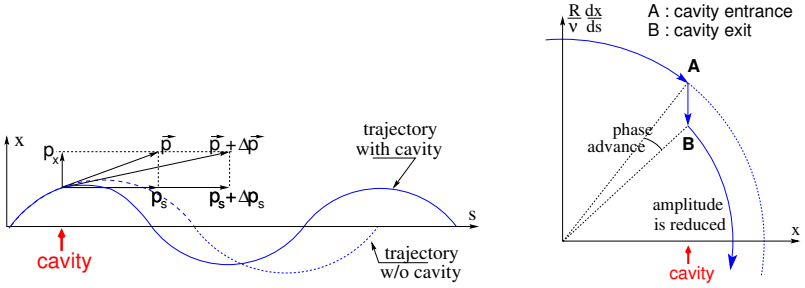

Fig. 1.6 Adiabatic damping of betatron oscillations ($\frac{\Delta p}{p} > 0$), here from $x'_{in} = p_x/p_s$ before the cavity, to $x'_{out} = p_x/(p_s + \Delta p_s)$ after the cavity. In the horizontal phase space, to the right, $\downarrow \Delta\left(\frac{dx}{ds}\right)$ if $\frac{dx}{ds} > 0$, $\uparrow \Delta\left(\frac{dx}{ds}\right)$ if $\frac{dx}{ds} < 0$.

$\begin{cases} x_{out} = x_{in} \\ x'_{out} \approx \frac{p_x}{p_s}(1 - \frac{dp}{p}) = x'_{in}(1 - \frac{dp}{p}) \end{cases}$, hence the transfer matrix of the cavity,

$$[C] = \begin{bmatrix} 1 & 0 \\ 0 & 1 - \frac{dp}{p} \end{bmatrix} \tag{1.16}$$

its determinant is $1 - dp/p$, the system is non-conservative (the surface in phase space is not conserved). Assume one cavity in the ring and [T].[C] the one-turn matrix with origin at entrance of the cavity. Its determinant is $\det[T] \times \det[C] = \det[C] = 1 - \frac{dp}{p}$. For N turns the matrix is $([T][C])^N$, its determinant is $(1 - \frac{dp}{p})^N \approx 1 - N\frac{dp}{p}$. The surface of the beam ellipse is $\epsilon \times \det[T]_{turn} = \epsilon_0 - \epsilon\frac{dp}{p}$ thus $\frac{d\epsilon}{\epsilon} = -\frac{dp}{p}$, the solution of which is

$$\epsilon \times p = \text{constant}, \quad \text{or} \quad \beta\gamma\epsilon = \text{constant} \tag{1.17}$$

• Exercise 1.3.2-2 In SATURNE ring, launch a few tens of particles evenly distributed on an initial invariant $\beta\gamma\epsilon = 10^{-6}\pi$m. Track them for a few hundred of turns as they are accelerated (use the same, artificial quasi-zero frequency cavity for identical longitudinal boost to all particles at each traversal). Plot the evolution of the surface of that ellipse with turn number, check against Eq. 1.17. Do it for both planes, horizontal and vertical. •

1.4 Synchrotron motion

By "synchrotron motion", or "phase oscillations", it is meant a mechanism that stabilizes the longitudinal motion of a particle around a synchronous phase, in virtue of

(i) the presence of a cavity with its frequency indexed on the revolution time (Sec. 1.4.1),

(ii) with the bunch centroid positioned either on the rising slope of the oscillating voltage (low energy regime), or on the falling slope (high energy regime) (Sec. 1.4.2).

1.4.1 *The synchronous particle*

The synchronous (or "ideal") particle follows the equilibrium trajectory around the ring (the reference closed orbit, about which all other particles will undergo a betatron oscillation) and its velocity satisfies

$$\mathrm{B}\rho = \frac{\mathrm{p}}{\mathrm{q}} = \frac{\mathrm{mv}}{\mathrm{p}} \rightarrow \mathrm{v} = \frac{\mathrm{qB}\rho}{\mathrm{m}}$$

- the revolution time is $\mathrm{T_{rev}} = \frac{2\pi\mathrm{R}}{\mathrm{v}} = \frac{2\pi\mathrm{R}}{\beta\mathrm{c}} = \frac{2\pi\mathrm{R}}{\mathrm{qB}\rho/\mathrm{m}}$
- the angular revolution frequency follows the increase of B:

$$\omega_{\mathrm{rev}} = \frac{2\pi}{\mathrm{T_{rev}}} = \frac{\mathrm{qB}\rho}{\mathrm{mR}}$$

- during the acceleration B(t) increases at a rate $\frac{\mathrm{dB}}{\mathrm{dt}} = \dot{\mathrm{B}}$, normally of the order of a Tesla/second.
- in order for the ideal particle to stay on that very closed orbit during the acceleration, its changing momentum must at all time satisfy $\mathrm{B(t)}\rho = \mathrm{p(t)/q}$. This defines p(t) as a function of B(t). The following B dependence of mass and angular frequency results:

$$\mathrm{m(t)} = \gamma(\mathrm{t})\mathrm{m_0} = \frac{\mathrm{q}\rho}{\mathrm{c}}\sqrt{\left(\frac{\mathrm{m_0}}{\mathrm{qc}\rho}\right)^2 + \mathrm{B(t)}^2},\ \ \omega_{\mathrm{rev}}(\mathrm{t}) = \frac{\mathrm{c}}{\mathrm{R}}\frac{\mathrm{B(t)}}{\sqrt{\left(\frac{\mathrm{m_0}}{\mathrm{qc}\rho}\right)^2 + \mathrm{B(t)}^2}}$$

- the RF voltage frequency $\omega_{\mathrm{RF}}(\mathrm{t}) = \mathrm{h}\omega_{\mathrm{rev}}(\mathrm{t})$ follows B(t), this maintains the synchronous phase at a fixed value
- over a turn the gain in energy is $\Delta\mathrm{W} = 2\pi\mathrm{q}\rho\mathrm{R}\dot{\mathrm{B}}$, the reference particle experiences a voltage $\mathrm{V} = \Delta\mathrm{W/q} = 2\pi\rho\mathrm{R}\dot{\mathrm{B}}$.

1.4.2 *Phase stability*

The voltage at the cavity at time t is

$$\mathrm{V} = \hat{\mathrm{V}}\sin\int\omega_{\mathrm{RF}}(\mathrm{t})\mathrm{t} = \hat{\mathrm{V}}\sin\phi(\mathrm{t}) \tag{1.18}$$

ω and possibly $\hat{\mathrm{V}}$ are slowly varying with time. On an harmonic h of the revolution frequency, ϕ explores the interval $2\pi\mathrm{h}$ over a turn (Fig. 1.7).

The synchronous (*aka* "ideal") particle presents itself at the cavity at the synchronous phase ϕ_s, the same at every turn, and experiences an energy gain

$$\Delta W = q\hat{V}\sin\phi_s \quad \text{thus} \quad \sin\phi_s = \frac{\Delta W}{q\hat{V}} = \frac{2\pi\rho R\dot{B}}{\hat{V}} \tag{1.19}$$

It results that there is a minimum voltage to apply to the cavity, for the synchronous particle to exist ($|\sin\phi_s| < 1$),

$$\hat{V} \geq 2\pi\rho R\dot{B}$$

The stability mechanism is illustrated in Fig. 1.7:

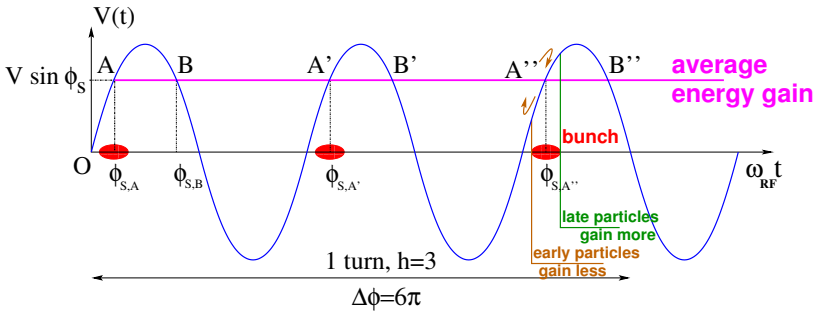

Fig. 1.7 Mechanism of phase stability, "longitudinal focussing". Below transition, $\gamma < \gamma_{tr}$, $\eta > 0$, acceleration occurs for a stable synchronous phase $\in]0, \pi]$, at A, A', A" in this illustration: a particle with higher energy goes around the ring quicker than synchronous particle, it arrives earlier (at $\phi < \phi_{s,A}$), it will experience a lower voltage than the synchronous particle and will progress towards the latter, in energy and in phase. A particle with lower energy takes more time, it arrives later, at $\phi > \phi_{s,A}$, it will experience a greater voltage than the synchronous particle. Beyond transition, $\gamma > \gamma_{tr}$, $\eta < 0$, the stable phase $\in [\pi, 2\pi[$, at B, B', B" here, with a similar stabilizing mechanism: a particle which is less energetic than the synchronous particle arrives earlier, $\phi < \phi_{s,B}$, and it sees a higher voltage, and inversely for a particle which is more energetic.

At high energy (think *very high*, $v \approx c$) an excess $\Delta p > 0$ only causes small change in velocity, whereas the average orbit radius does increase (following $\Delta R/R_0 = \alpha\Delta p/p_0$), thus a more energetic particle takes longer than the synchronous particle to complete a turn, it arrives later at the cavity (at $\phi > \phi_s$), thus *it has to* see a smaller voltage in order slow down and catch up with the synchronous particle: the appropriate working point is at B. At low energy (think *very* low), the relative excess in velocity for a particle having an excess Δp, is greater than the relative increase in orbit radius, the off-momentum particle takes less time to perform a turn, it arrives at the cavity ahead of time (at $\phi < \phi_s$), thus *it has to* see a lower

voltage in order to catch up (increase its revolution time), thus the working point has to be at A.

Quantifying that, by differentiation of $\omega = 2\pi/\mathrm{T}$ (with $\mathrm{T} = \mathcal{L}/\mathrm{v} \Rightarrow -\frac{\mathrm{dT}}{\mathrm{T}} = \frac{\mathrm{dv}}{\mathrm{v}} - \frac{\mathrm{d}\mathcal{L}}{\mathcal{L}}$ and $\frac{\mathrm{d}\mathcal{L}}{\mathcal{L}} = \alpha\frac{\mathrm{dp}}{\mathrm{p}}$):

$$\frac{\mathrm{d}\omega}{\omega} = -\frac{\mathrm{dT}}{\mathrm{T}} = (\frac{1}{\gamma^2} - \alpha)\frac{\mathrm{dp}}{\mathrm{p}} = (\frac{1}{\gamma^2} - \frac{1}{\gamma_{\mathrm{tr}}^2})\frac{\mathrm{dp}}{\mathrm{p}} \quad \text{or} \quad \frac{\mathrm{d}\omega}{\omega} = \eta\frac{\mathrm{dp}}{\mathrm{p}}$$

The change in phase focusing regime occurs at the "transition γ"

$$\text{"phase} - \text{slip"} \text{ factor value } \eta = 0, \quad \gamma_{\mathrm{tr}} = 1/\sqrt{\alpha}$$

If the lattice transverse focusing optics has γ_{tr} somewhere in the acceleration range, then the RF phase is quickly shifted at the time of the transition during the acceleration, from A to B (Fig. 1.7), this is achieved without beam loss. This is the case at BNL's AGS, RHIC injector; at CERN's PS, LHC injector chain.

For weak focusing machines (see the Cyclotron Chapter), one has $\alpha \approx 1/\nu_{\mathrm{x}}^2$, thus $\gamma_{\mathrm{tr}} \approx \nu_{\mathrm{x}}$. Some synchrotrons present the property of an "imaginary γ_{tr}", the transition does not exist, this is the case when the lattice optics achieves $\alpha < 0$.

• Exercise 1.4-1 What is the value of the transition γ in SATURNE 1? Verify by tracking: check the longitudinal stability when accelerating a proton, either on the rise slope (A), or the falling slope (B) of the RF. •

1.4.3 *Synchrotron oscillations*

There are h equilibrium positions ϕ_{s} over a revolution period. In the illustration of Fig. 1.7 for instance, case h=3, acceleration occurs at

- at A, A', A" if $\gamma < \gamma_{\mathrm{tr}}$,
- at B, B', B" if $\gamma > \gamma_{\mathrm{tr}}$.

All particles located in the vicinity of these points will undergo a stable oscillatory motion, a "phase oscillation", centered on the respective ϕ_{s}. Thus h bunches can circle around the ring, with an angular frequency which is that of the synchronous particle, they are $2\pi/\mathrm{h}$ distant in phase (and in azimuth around the ring).

Particles with small amplitude motion, $\Delta\phi \ll \pi/2$ undergo an harmonic motion with frequency

$$\Omega_{\mathrm{s}} = \frac{\mathrm{c}}{\mathrm{R}}\sqrt{\frac{\mathrm{h}\eta\cos\phi_{\mathrm{s}}\mathrm{q}\hat{\mathrm{V}}_{\mathrm{RF}}}{2\pi\mathrm{E_s}}} \qquad \begin{cases} \mathrm{E_s} = \mathrm{m}\gamma_{\mathrm{s}} = \text{synchronous energy} \\ \mathrm{R} = \text{circumference}/2\pi \end{cases} \tag{1.20}$$

solution of

$$\frac{\mathrm{d}^2\phi}{\mathrm{dt}^2} + \Omega_\mathrm{s}^2 \Delta\phi = 0 \quad (\Delta\phi = \phi - \phi_\mathrm{s}) \tag{1.21}$$

The number of synchrotron oscillations per turn, the "synchrotron tune" is

$$\mathrm{Q_s} = \frac{\Omega_\mathrm{s}}{\omega_\mathrm{s}} \tag{1.22}$$

with ω_s the revolution frequency of the synchronous particle (in a similar manner to the transverse tunes, $\nu_\mathrm{x} = \omega_\mathrm{x}/\omega_\mathrm{s}$, Eq. 1.11).

Large amplitude motion satisfies the more general equation

$$\frac{\mathrm{d}^2\phi}{\mathrm{dt}^2} + \frac{\Omega_\mathrm{s}^2}{\cos\phi_\mathrm{s}}(\sin\phi - \sin\phi_\mathrm{s}) = 0 \tag{1.23}$$

The natural coordinate system for the longitudinal phase space comes out to be $(\phi, \dot{\phi})$, however the particle coordinate actually tracked is its momentum p, thus the longitudinal phase space usually is $(\phi, \Delta\mathrm{p})$. Both are related by

$$\Delta\mathrm{p} = -\frac{\mathrm{p_s}}{\mathrm{h}\eta\omega_\mathrm{s}}\dot{\phi} \tag{1.24}$$

• Exercise 1.4.3-1. "Stationary bucket".
In SATURNE ring, now install the RF system model (use a cavity model with self-computed RF frequency, $\mathrm{f_{RF}}$ in Eq. 1.19), complete your spreadsheet with the RF motion parameters accordingly (phase-slip factor, RF frequency, voltage, Ω_s, etc.).
1.a - Take $\phi_\mathrm{s} = 0$, track a particle with small amplitude motion, both transverse and longitudinal (take for instance zero vertical invariant), over a few thousand turns.
1.b - Plot its motion in the longitudinal phase space $(\Delta\mathrm{p}, \phi)$, superimpose the theoretical solution of Eq. 1.21.
1.c - Determine the motion frequency Ω_s, in two different ways:
(i) from the number of turns around the ring, over one phase oscillation
(ii) from Fourier analysis. •

• Exercise 1.4.3-2. "Accelerated bucket".
Take SATURNE ring and RF system as of of Exercise 1.4.3-1.
2.a - Take instead $\phi_\mathrm{s} = 30$ degrees, track a particle with small amplitude motion, both transverse and longitudinal, over a few thousand turns. Start for instance from SATURNE injection energy.
2.b - Plot its motion in the longitudinal phase space $(\Delta\mathrm{p}, \phi)$, superimpose the theoretical solution of Eq. 1.21.

2.c - Determine the motion frequency in longitudinal phase space, Ω_s, in two different ways:

(i) from the number of turns around the ring, over one phase oscillation

(ii) from Fourier analysis. •

• Exercise 1.4.3-3.

Take SATURNE ring as of Exercise 1.4.3-2.

3.a - Calculate the theoretical RF frequency law from injection to top energy, superimpose with the very quantity out of the self-computation outcomes of the previous RF computer model.

3.b - Replace the previous RF system (Ex. 1.4.3-1) with a computer model that allows following that external law. Re-compute the quantities of Ex. 1.4.3-1, have the results from the two methods (self-computed f_{RF} and the present readout technique) coincide. •

• Exercise 1.4.3-4. "Separatrix".

Take SATURNE ring as of Exercise 1.4.3-2, synchronous RF phase set to $\phi_s = 30$ degrees, ready for single-particle tracking.

4.a - Slowly push (by small iterations on initial Δp values for instance) the longitudinal motion amplitude to its maximum stable value: below, the motion is oscillatory, beyond it is unbounded.

4.b - Once there, generate the separatrix of the RF motion: the limit between harmonic motion, and unbounded motion. Plot particle trajectories in the longitudinal phase space for a few different values of Δp in the region of the stability limit. •

1.4.4 *RF bucket*

• Exercise 1.4.4-1.

1.a - By tracking, show that the bucket height, "momentum acceptance", satisfies

$$\pm \frac{\Delta p}{p} = \pm \frac{1}{\beta} \sqrt{\frac{q\hat{V}}{\pi h \eta E_s} \left[-(\pi - 2\phi_s) \sin \phi_s + 2 \cos \phi_s \right]} \tag{1.25}$$

1.b - Show that the maximum extent in phase for small amplitude oscillations, from the tracking, satisfies

$$\pm \Delta\phi_{max} = \frac{h \eta E_s}{p_s R_s \Omega_s} \times \text{Max.} \left(\frac{\Delta E}{E_s} \right) \tag{1.26}$$

1.c - Show that tracking and theory agree on the bucket length and height, taking some ϕ_s values in $[0, 2\pi]$. •

1.5 Bibliography

[1.a] V. Veksler, A new method of acceleration of relativistic particles, J. of Phys. USSR 9 153-158 (1945), Translation L. Bell in [2].
[1.b] E.M. McMillan, The Synchrotron, Phys. Rev. 68 143-144 (1945).

[2] R. Barlow et al., EMMAThe worlds first non-scaling FFAG, NIM A Volume 624, Issue 1, 1 December 2010, Pages 1-19.

[3] E. Yamakawa et al., Serpentine acceleration in zero-chromatic FFAG accelerators, Nuclear Instruments and Methods in Physics Research A, Volume 716, p. 46-53.
[4] Bruck H., Debraine P., Levy-Mandel R., Lutz J., Podliasky I., Prevot F., Taieb J., Winter S.D., Maillet R., Caractéristiques principales du Synchrotron Protons de Saclay et résultats obtenus lors de la mise en route, rapport CEA no.93, CEN-Saclay, 1958.
[5] The ZGS, ANL web site.
[6] M. Froisaart and R. Stora, Nucl. lnst. Meth. 7 (l960) 297.
[7] Andre Tkatchenko, Review of polarized hadron beams, Procs. EPAC 90 Accel. Conf.
[8] T. Khoe et al., Acceleration of polarized protons to 8.5 GeV/c, Particle Accelerators, 1975, Vol. 6, pp. 213-236.
[9] G. Leleux, Circular accelerators, INSTN lectures, SATURNE Laboratory, CEA Saclay (Juin 1978). Some passages of the present document are inspired from these lectures.
[10] H. Bruck, Circular particle accelerators, English translation.